Science & Technology Development Journal – Engineering and Technology 2023, 6(4):2048-2059

Open Access Full Text Article

Research article

Neural adaptive sliding mode with RBF applied in PMSM

Nguyen Tien Dat[1,2], Ho Pham Huy Anh[1,2,*]

ABSTRACT

In practical applications, permanent magnet synchronous motors's benefits over brush-type motors, such as compact designs, high torque to inertia ratio, high power density, high air-gap flux density, and high efficiency. Moreover, they are also increasingly replacing induction motors in a variety of fields of application. Fast reaction, accurate control, and minimal overshoot feature represent crucial installation considerations while developing a control system for permanent magnet synchronous motors applications. Permanent magnet synchronous motor models are nonlinear and high-order concerning time-varying parameters, so a suitable controller is required. One well-known resilient model base control technique for systems with parameter fluctuations and outside disturbances is sliding mode control. First, the sliding-mode controller is employed to reduce chattering and stabilize the PMSM drive system. On the other hand, modifications to the drive system's configuration and external disturbances might totally destroy the control performance. Therefore, this paper investigates combining neural networks with the sliding mode technique to propose an advanced robust permanent magnet synchronous motors velocity control algorithm. In order to increase the robustness and stability and decrease sliding mode chattering of the controller, our goal is to showcase several adaptive law designs for updating online sliding mode control laws and composite controller designs using radial basis function neural networks. The suggested adaptive neural network sliding mode controller based on the field-oriented scheme ANSMC-FOC technique, also known as the adaptive neural sliding mode based on a field-oriented control approach, confirms its complete accuracy and achieves outperforming control performance compared to PID and classical sliding mode control methods. Thus, the proposed permanent magnet synchronous motors velocity control algorithm is convincingly better than other permanent magnet synchronous motors' advanced speed control approaches.

Key words: SMC Technique, PMSM Motor, FOC Control, RBF Neural Model, adaptive Proportional Integral (PI) control, Adaptive Neural SMC (ANSMC-FOC/ ANSMC) control

[1]*Ho Chi Minh City University of Technology (HCMUT), 268 Ly Thuong Kiet Street, District 10, Ho Chi Minh City, Viet Nam*

[2]*Vietnam National University Ho Chi Minh City (VNU-HCM), Linh Trung Ward, Thu Duc District, Ho Chi Minh City, Viet Nam*

Correspondence

Ho Pham Huy Anh, Ho Chi Minh City University of Technology (HCMUT), 268 Ly Thuong Kiet Street, District 10, Ho Chi Minh City, Viet Nam

Vietnam National University Ho Chi Minh City (VNU-HCM), Linh Trung Ward, Thu Duc District, Ho Chi Minh City, Viet Nam

Email: hphanh@hcmut.edu.vn

History

- Received: 07-12-2022
- Accepted: 27-3-2024
- Published Online: 13-5-2024

DOI :

https://doi.org/10.32508/stdjet.v6i4.1057

INTRODUCTION

The permanent magnet synchronous motor with excellent characteristics such as a straightforward structure, a small footprint, a high power factor, and incredible precision was created in 1980. Due to the benefits above, PMSM is gradually displacing DC and asynchronous motors in electric vehicles. The PMSM motor has a lot of cross-sectional effects that depend on time; therefore, to fully utilize its potential, a proper controller must be designed. There are now two primary ways to regulate PMSM motors: FOC and direct force DTC control[1]. The DTC technique directly handles the IGBT's on-off switch, whereas the FOC control calls for the current approach. Designing a PMSM controller that can deal with complex system architecture and environmental impacts is both a requirement and a difficulty. In some experiments, the PID classic controller regulates motor speed. The research employs the self-tuning PID set to address the issue above because the PID set with preset parameters is only appropriate for one type of control situation[2–5]. Much research has also been conducted via using of advanced control methods, such as sliding mode controllers[6,7], adaptive fuzzy[8], and NN-based applications[9,10]. Authors Xi et al. (2005)[11] regulated PMSM motor speed with a self-tuning PID. Zhang, et al.[12] created a slip control approach for PMSM velocity regulation by proposing an estimator to enhance the PMSM velocity precision regardless of plant perturbations. Li et al.[13] introduced an advanced internal IMC method to regulate the PMSM motor velocity.

Multiple kinds of different research on advanced PMSM motor speed regulation methods have recently been conducted. For instance, authors[14] suggest observation diagrams based on a control diagram and a neural network through which an effective sensor-free optimization for noisy and saturation voltage permanent-magnet synchronous motors is researched. The PMSM drive system is subjected to a novel vector-based controller via a new

Cite this article : Dat N T, Anh H P H. **Neural adaptive sliding mode with RBF applied in PMSM**. *Sci. Tech. Dev. J. – Engineering and Technology* 2023; 6(4):2048-2059.

measured erroneous approach [15]. The suggested control structure can identify common current-sensing signal defects such as discontinuous signal, missing returned signal, fluctuating gain, and significant external noise. In other research, the permanent magnet synchronous motor transmission system running at high speed is proposed to be controlled by an adaptively optimized super-twisting SMC control approach [16]. Junejo et al. [17] suggested a novel adaptive terminal SMC reaching rule to decrease input control efforts by dynamically adopting all favorable qualities regarding finite time convergence, high tracking accuracy, and chattering in the system's control input. For various driving situations, the finite control set model predictive control gives an enhanced dynamic response and a superior steady-state response [18]. Recently Shanthi [19] (2021) suggested adaptive neuro-fuzzy-dependent findings and proved they are transiently efficient. The robustness of adaptive neuro-fuzzy PID and SMC-PID control methods has shown good regarding simple settled time, null-peak transient, and null steady-state erroneous value.

Recently, the efficiency and the promising potential of adaptive PI-based disturbance observers and controllers in PMSM speed control have increasingly attracted the attention of researchers. The authors offered a unique disturbance rejection control technique in which the suggested adaptive DR-PI control technique was practicable with an affordable gain tuning rule for PMSM control [20]. Continually, the authors [21] (2022) successfully introduced an integrating disturbance observer-based control combined with an active disturbance rejection control for the PMSM speed control which is based on an adaptive PI approach for enhancing both PMSM performance and robustness. Apart from this method, a comprehensive high-order fuzzy-PI observer [22] for computing the total disturbance of PMSM motors, including disturbance rejection and high-performance speed tracking has been initiatively suggested. Moreover, an adaptive PI-PI control technique for PMSM [23] is improved by using high-order PI-PI disturbance observer-based control regardless of disturbance and unmodeled dynamics.

Inspired by the results above-mentioned, this study thoroughly examines and verifies the combination of adaptive SMC with RBF technique applied in PMSM control strategy using the previously referred PMSM velocity control research. The rest of this study is structured with following sections. The section 2 presents the methodology which includes the PMSM model is presented in Section 2.1 and Section 2.2 introduces the suggested SMC for the PMSM utilizing RBF neural technique. Section 3 shows the outcomes of PMSM velocity regulation applying the suggested control system. The conclusions will be given in Section 4.

METHODOLOGY

PMSM MATHEMATICAL MODELLING

Suppose the magnetic circuit represents unsaturated and the magnetic field is distributed sine-wave. The frame below displays the PMSM mathematical model under the conditions above:

$$\begin{aligned}
\frac{di_d}{dt} &= \frac{1}{L_d}u_d - \frac{R_s}{L_d}i_d + \omega_m i_q \frac{L_q}{L_d}n_p \\
\frac{di_q}{dt} &= \frac{1}{L_q}u_q - \frac{R_s}{L_q}i_q + \omega_m i_q \frac{L_d}{L_q}n_p - \frac{\lambda n_p \omega_m}{L_q} \\
\frac{d\omega_m}{dt} &= \frac{1}{J}\left(T_e - T_1 - F\omega_m\right) \\
T_e &= \frac{3}{2}n_p\left[\lambda i_q + \left(L_d - L_q\right)i_d i_q\right]
\end{aligned} \tag{2.1}$$

Where u_d, u_q represent the voltage values in dq-coordinate; i_d, i_q denote the current components in dq-coordinate; L_d, L_q denote inductance elements in dq-coordinate; R_s represents stator resistance; ω_m represents PMSM shaft velocity; eventually T_l, n_p, F, J represent load moment, poles' number, viscous parameter and PMSM inertial torque, respectively.

The PMSM description uses a 3rd-oder mathematical scheme regarding components, PMSM velocity ω_m, and control voltage elements u_d, u_q. In $dq0$ coordination, such PMSM model is as follows:

$$\begin{aligned}
\dot{x}_1 &= \frac{1}{L_d}u_d - \frac{R_s}{L_d}x_1 + x_3 x_2 \frac{L_q}{L_d}n_p \\
\dot{x}_2 &= \frac{1}{L_q}u_q - \frac{R_s}{L_q}x_2 - x_3 x_1 \frac{L_d}{L_q}n_p - \frac{\lambda n_p x_3}{L_q} \\
\dot{x}_3 &= \frac{1}{J}\left(\frac{3}{2}n_p\left[\lambda x_2 + \left(L_d - L_q\right)x_1 x_2\right]\right. \\
&\left. - T_1 - F\omega_m\right) \\
y_1 &= x_3 \\
y_2 &= x_1
\end{aligned} \tag{2-2}$$

In which control variables u_d, u_q and $x_1 = i_d$, $x_2 = i_q$, $x_3 = \omega_m$

SUGGESTED ADAPTIVE RBF-NEURAL SMC CONTROL METHOD

The PMSM driving system is described with respect to the rotor as follows:

$$\begin{aligned}
\frac{di_d}{dt} &= \frac{1}{L_d}u_d - \frac{R_s}{L_d}i_d + \omega_m i_q \frac{L_q}{L_d}n_p \\
\frac{di_q}{dt} &= \frac{1}{L_q}u_q - \frac{R_s}{L_q}i_q - \omega_m i_d \frac{L_d}{L_q}n_p - \frac{\lambda n_p \omega_m}{L_q} \\
\frac{d\omega_m}{dt} &= \frac{1}{J}\left(T_e - T_l - F\omega_m\right)
\end{aligned} \tag{2-3}$$

Where $T_e = \frac{3}{2}n_p\left[\lambda i_q + \left(L_d - L_q\right)i_d i_q\right]$

In addition to the current controller created using the FOC method, let us develop a PMSM velocity control block.

At first due to $L_d = L_q$ it gives:

$$\frac{d\omega_m}{dt} = \frac{1}{J}\left(\frac{3}{2}n_p\left[\lambda i_q\right] - T_l - F\omega_m\right) \quad (2\text{-}4)$$

From (2-4), we develop a novel adaptive RBF-SMC control method for accurately regulating the PMSM velocity.

Consider $x_1 = \omega_m$; $u = i_q$ (2-5) will be derived as follows:

$$\begin{cases} \dot{x}_1 = \frac{1}{J}\left(\frac{3}{2}n_p\left[\lambda u\right] - T_l - Fx_1\right) \\ y = x_1 \end{cases} \quad (2\text{-}5)$$

Based on the SMC control approach, we have $\dot{y} = a(x) + b(x)u$ with $a(x) = \frac{1}{J}(-T_l - Fx_1)$ and $b(x) = \frac{1}{J}\left(\frac{3}{2}n_p\lambda\right)$

However, the slide controller cannot be implemented due to unknown equations $a(x)$ $b(x)$. The problem here is to identify the control law by online identification and calculating the control law based on that result u; this is called indirect adaptive control.

$$\begin{cases} u_{ce} = b^{-1}(x)(-a(x) + v(t)) \\ v(t) = \dot{y}_m + Ksign(s) \end{cases} \quad (2\text{-}6)$$
$$with\ s = e = y_m - y$$

Then a new adaptive RBF-SMC control approach was proposed to estimate equations $\widehat{a}(x)$;$\widehat{b}(x)$ along with computing the control law in (2-7):

$$u_{ce} = \widehat{b}^{-1}(x)(-\widehat{a} + v(t)) \quad (2\text{-}7)$$

The $\widehat{a}(x)$;$\widehat{b}(x)$ in (2-7) denotes the RBF model which includes three basic equations in hidden-layer used to estimate $\widehat{a}(x)$;$\widehat{b}(x)$ as presented in (2-8):

$$\begin{cases} \widehat{a}(x) = \theta_a^T \xi_a(x) \\ \widehat{b}(x) = \theta_b^T \xi_b(x) \end{cases} \quad (2\text{-}8)$$

with θ_a, θ_b represent neuron weighting vectors. These coefficients will be adjusted adaptively in real-time to ensure the optimum magnitude $\theta_a \to \theta_a^*$, $\theta_b \to \theta_b^*$ as for $\widehat{a}(x) \to a(x)$, $\widehat{b}(x) \to b(x)$..

Select $\begin{cases} \theta_a = \begin{bmatrix} \theta_{1a} & \theta_{2a} & \theta_{3a} \end{bmatrix} \\ \theta_b = \begin{bmatrix} \theta_{1b} & \theta_{2b} & \theta_{3b} \end{bmatrix} \end{cases}$

$$\begin{cases} \xi_a(x) = \begin{bmatrix} \xi_{a1}(x) & \xi_{a2}(x) & \xi_{a3}(x) \end{bmatrix} \\ \xi_b(x) = \begin{bmatrix} \xi_{b1}(x) & \xi_{b2}(x) & \xi_{b3}(x) \end{bmatrix} \end{cases} \quad (2\text{-}9)$$

where the primary equation is selected as $\xi(x) = e^{-\frac{\left[(x-\mu)^2\right]}{\sigma^2}}$. The chosen RBF functions ensure uniformity in the state region and presented in Figure 1.

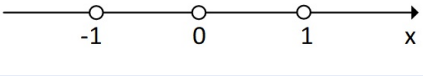

Figure 1: Design of the RBFNN centre

Here σ parameter of RBF functions is equally selected $\sigma = -0.6$.

$$\begin{cases} \theta_a^* = arg\min\limits_{\theta_a \in \Omega_a}\left\{sup\limits_{x \in S_x}|\theta_a^T \xi_a - a(x)\right\} \\ \theta_b^* = arg\min\limits_{\theta_b \in \Omega_b}\left\{sup\limits_{x \in S_x}|\theta_b^T \xi_b - b(x)\right\} \end{cases} \quad (2\text{-}10)$$

When all coefficients are updated in real-time, the structural error is a structural difference between the identified and accurate models. Currently, the difference of the designed model with the real one is defined as follows:

$$\begin{cases} a(x) = \theta_a^* \xi_a + \delta_a(x) \\ b(x) = \theta_b^* \xi_b + \delta_b(x) \end{cases} \quad (2\text{-}11)$$

where $\delta_a(x)$, $\delta_b(x)$ represent the structure erroneous values in comparison with the ideal RBF through which, the erroneous values between the estimated RBF with the ideal model described in (2-12):

$$\begin{cases} \widehat{a}(x) - a(x) = \widetilde{\theta}_a^T \xi_a - \delta_a - \delta_a(x) \\ \widehat{b}(x) - b(x) = \widetilde{\theta}_b^T \xi_b - \delta_b - \delta_b(x) \end{cases} \quad (2\text{-}12)$$

We have:

$$\begin{aligned} \dot{y} &= a(x) + b(x)\left[u_{ce} + u_{si}\right] \\ &= \widehat{a}(x) - \widehat{a}(x) + \widehat{b}(x)u_{ce} - \widehat{b}(x)u_{ce} \\ &+ a(x) + b(x)\left[u_{ce} + u_{si}\right] \\ &= \widehat{a}(x) + \widehat{b}(x)u_{ce} - \left[\widehat{a}(x) - a(x)\right] \\ &- \left[\widehat{b}(x) - b(x)\right]u_{ce} + b(x)u_{si} \\ &= v(t) - \left[\widehat{a}(x) - a(x)\right] - \left[\widehat{b}(x) - b(x)\right]u_{ce} \\ &+ b(x)u_{si} \end{aligned} \quad (2\text{-}13)$$

From (2-12) and (2-13), the following Lyapunov equation will be determined as:

$$\begin{aligned} \dot{s} &= \dot{y}_m - \dot{y} \\ &= \dot{y}_m - \left[v(t) - \left[\widehat{a}(x) - a(x)\right] - \left[\widehat{b}(x) - b(x)\right]u_{ce}\right. \\ &\left. + b(x)u_{si}\right] \\ &= -Ksign(s) + \left[\widehat{a}(x) - a(x)\right] + \left[\widehat{b}(x) - b(x)\right]u_{ce} \\ &- b(x)u_{si} \end{aligned} \quad (2\text{-}14)$$

Firstly this candidate is considered quadratic regarding tracking erroneous and parametric erroneous values described as follows:

$$V = \frac{1}{2}s^2 + \frac{1}{2}\widetilde{\theta}_a^T Q_a \widetilde{\theta}_a + \frac{1}{2}\widetilde{\theta}_b^T Q_b \widetilde{\theta}_b \quad (2\text{-}15)$$

$$\begin{aligned}\dot{V} &= s\dot{s} + \widetilde{\theta}_a^T Q_a \dot{\widetilde{\theta}}_a + \widetilde{\theta}_b^T Q_b \dot{\widetilde{\theta}}_b \\ &= \left[-Ksign(s) + [\widehat{a}(x) - a(x)] + \left[\widehat{b}(x) - b(x)\right] u_{ce}\right. \\ &\left. -b(x) u_{si}\right] s + \widetilde{\theta}_a^T Q_a \dot{\widetilde{\theta}}_a + \widetilde{\theta}_b^T Q_b \dot{\widetilde{\theta}}_b \\ &= \left[-Ksign(s) + \widetilde{\theta}_a^T \xi_a - \delta_a(x) + \left[\widetilde{\theta}_b^T \xi_b(x)\right] u_{ce}\right. \\ &\left. -b(x) u_{si}\right]_s + \widetilde{\theta}_a^T Q_a \dot{\widetilde{\theta}}_a + \widetilde{\theta}_b^T Q_b \dot{\widetilde{\theta}}_b \qquad (2-16) \\ &= sKsign(s) + s(-\delta_a(x) - \delta_b(x) u_{ce}) \\ &+ \widetilde{\theta}_a^T \left(\xi_a s + Q_a \dot{\theta}_a\right) + \widetilde{\theta}_b^T \left(\xi_b u_{ce} s + Q_b \dot{\theta}_b\right) \\ &- b(x) u_{si} s\end{aligned}$$

Choose the adapted coefficient rule as:

$$\begin{cases} \dot{\theta}_a = -Q_a^{-1} \xi_a s \\ \dot{\theta}_b = -Q_b^{-1} \xi_a u_{ce} s \end{cases} \qquad (2\text{-}17)$$

Then

$$\begin{aligned}&\dot{V} = -sKsign(s) + s(\delta_a(x) + \delta_b(x) u_{ce}) \\ &-b(x) u_{si} s \le -sKsign(s) + \\ &|s|(|\delta_a(x)| + |\delta_b(x)||u_{ce}|) - b(x) u_{si} s \qquad (2\text{-}18) \\ &\le -sKsign(s) + |s|\left(\overline{\delta_a(x)} + \overline{\delta_b(x)}|u_{ce}|\right) \\ &-b(x) u_{si} s\end{aligned}$$

Ensuring the structure erroneous value inside the predetermined bounds, choose the sliding SMC element such that $\dot{V} < 0$. Then from (2-18), it gives:

$$u_{si} = \frac{1}{\underline{b(x)}}\left(\overline{\delta_a(x)} + \overline{\delta_b(x)}|u_{ce}|\right) sign(s) \qquad (2\text{-}19)$$

Where $\overline{\delta_a(x)}, \overline{\delta_b(x)}|$ represent upper bounds of parametric erroneous values and $\underline{b(x)}$ represents the lower limit of .

$$\begin{aligned}&\dot{V} \le -sKsign(s) + |s|\left(\overline{\delta_a(x)} + \overline{\delta_b(x)}|u_{ce}|\right) - \\ &b(x)\left[\frac{1}{\underline{b(x)}}\left(\overline{\delta_a(x)} + \overline{\delta_b(x)}|u_{ce}|\right) sign(s)\right] s \\ &\Leftrightarrow \dot{V} \le -sKsign(s) + |s|\left(\overline{\delta_a(x)} + \overline{\delta_b(x)}|u_{ce}|\right) - \\ &\frac{b(x)}{\underline{b(x)}}\left(\overline{\delta_a(x)} + \overline{\delta_b(x)}|u_{ce}|\right)|s| \\ &\Leftrightarrow \dot{V} \le -sKsign(s) \\ &-\left(\frac{b(x)}{\underline{b(x)}} - 1\right)\left(\overline{\delta_a(x)} + \overline{\delta_b(x)}|u_{ce}|\right)|s| \le 0 \qquad (2-20)\end{aligned}$$

The system is stable because V ensures an un-negative quadratic equation.

RESULTS AND DISCUSSIONS

In the dq0 domain, a three-phase synchronous motor is controlled using the FOC algorithm. The FOC divides the current vector into two parts, one for each component of the force and magnetic field. The goal of FOC control is to make sure $i_d = 0$. Because the entire amount of electrical energy in the stator is utilized to create the electric force, the motor driven by the FOC method is highly efficient and presented in Figure 2 and Figure 3.

The PMSM actual rotating velocity using ASMC well tracks the referential curve compared to 2 other comparative control techniques. Concerning ASMC, during an abruptly varying-load issues the PMSM's coefficients to be varied, the ASMC output perfectly adapts to these load variations. Then it keeps the real PMSM rotating velocity to accurately track the desired velocity.

with represent the parameters of the current i_d controller; *P2, I2* represent the parameters of the current i_q controller and *P3. I3* denote the parameters of the current ω_m controller. Figure 4 shows that systematic response survey response is affected by parameter PID changing as shown in Table 1.

Figure 5 shows that systematic response survey response is affected by parameter PID changing as shown in Table 2. Investigate the influence of controller parameters on response quality, then select the best control quality parameter set to implement on the microcontroller. Those experiments are carried out on simulation to choose the controller's parameter before applying the control feature on an actual test using formulas (2-7) and (2-19).

$$\begin{aligned}u_{ce} &= \widehat{b}^{-1}(x)(-\widehat{a}(x) + v(t)) \\ u_{si} &= \frac{1}{\underline{b(x)}}\left(\overline{\delta_a(x)} + \overline{\delta_b(x)}|u_{ce}|\right) sign(s)\end{aligned}$$

Figure 6 shows that the systematic response survey response is affected by the parameter Q_a^{-1}, Q_b^{-1} of the proposed controller changing as shown in Table 3. From the simulation, we conclude that the larger Q_a^{-1}, Q_b^{-1} the faster the system adapts.

Figure 7 shows that the systematic response survey response is affected by the parameter $\overline{\delta_a(X)}$, $\overline{\delta_b(X)}$ of the proposed controller changing as shown in Table 4. The sliding mode control component ensures the system's stability when an error occurs between the recognized and correct model structure. When the selection bounds are too small, the noise quickly affects the system. When the selection bounds are too large, chattering occurs as a result.

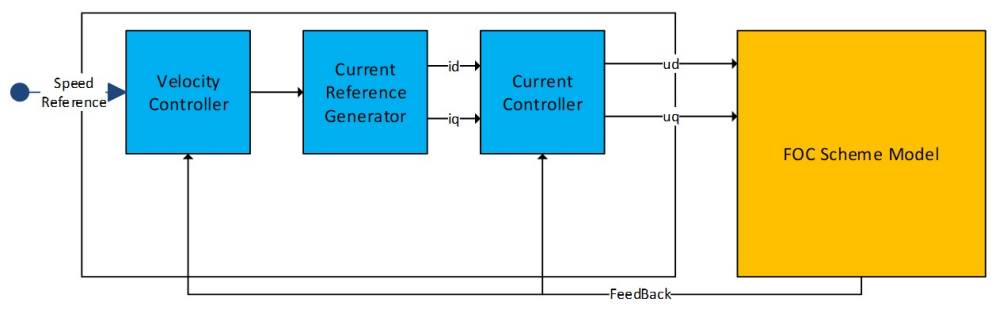

Figure 2: Experiment PMSM speed control block-diagram

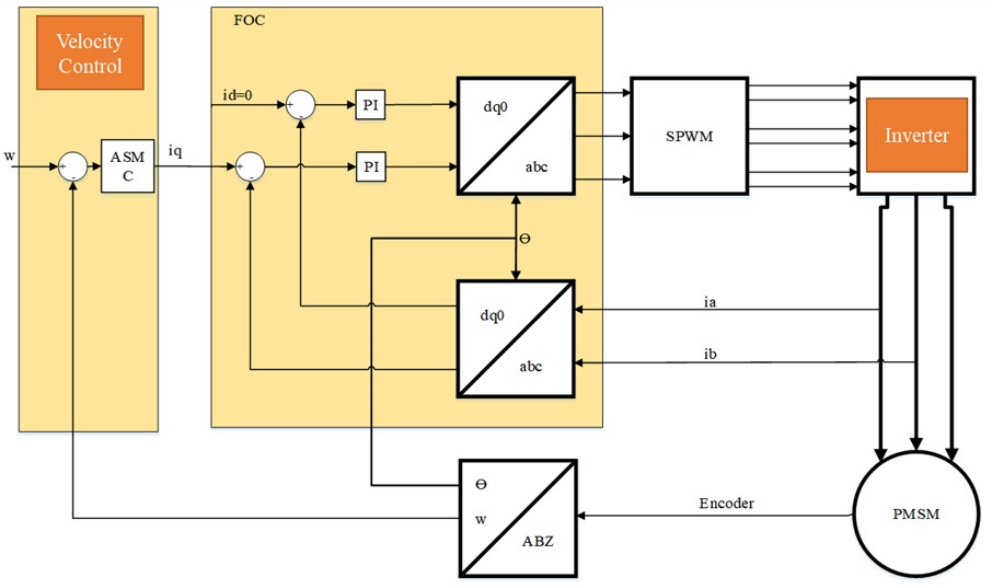

Figure 3: Experiment PMSM speed control block-diagram

Table 1: Systematic response survey table affected by parameter PID changing *P1, P2* as current control block

P1	P2	P3	I1	I2	I3
15	15	0.05	1	1	0.1
20	20	0.05	1	1	0.1
25	25	0.05	1	1	0.1
30	30	0.05	1	1	0.1
35	35	0.05	1	1	0.1

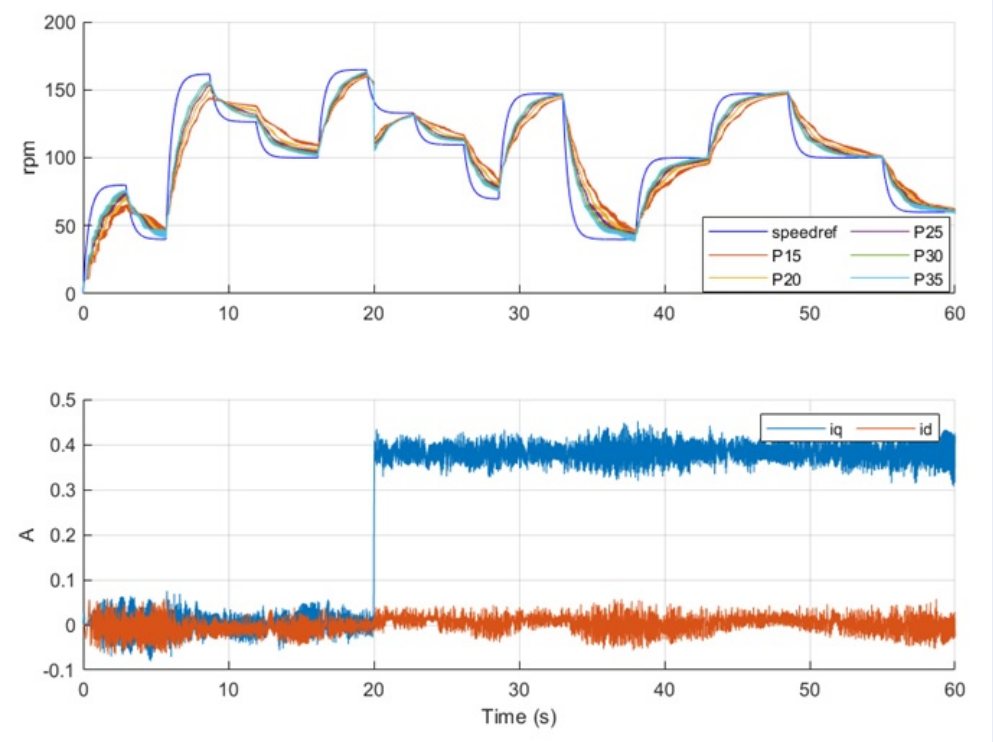

Figure 4: Systematic response survey response affected by parameter PID changing *P1, P2*

Table 2: Systematic response survey table affected by parameter PID changing P3 as speed control block

P1	*P2*	*P3*	*I1*	*I2*	*I3*
20	20	1/5	1	1	0.1
20	20	1/10	1	1	0.1
20	20	1/20	1	1	0.1
20	20	1/50	1	1	0.1
20	20	1/100	1	1	0.1

Table 3: Systematic response survey table affected by parameter Q_a^{-1}, Q_b^{-1}

TH TS	1	2	3	4	5
K_{pq}	20	20	20	20	20
K_{pd}	15	15	15	15	15
K_{iq}	2	2	2	2	2
K_{id}	1	1	1	1	1
Q_a^{-1}	10	25	50	75	100
Q_b^{-1}	10	25	50	75	100
$b(x)$	0.4	0.4	0.4	0.4	0.4
$\overline{\delta_a(X)}$	0.06	0.06	0.06	0.06	0.06
$\overline{\delta_b(X)}$	0.04	0.04	0.04	0.04	0.04

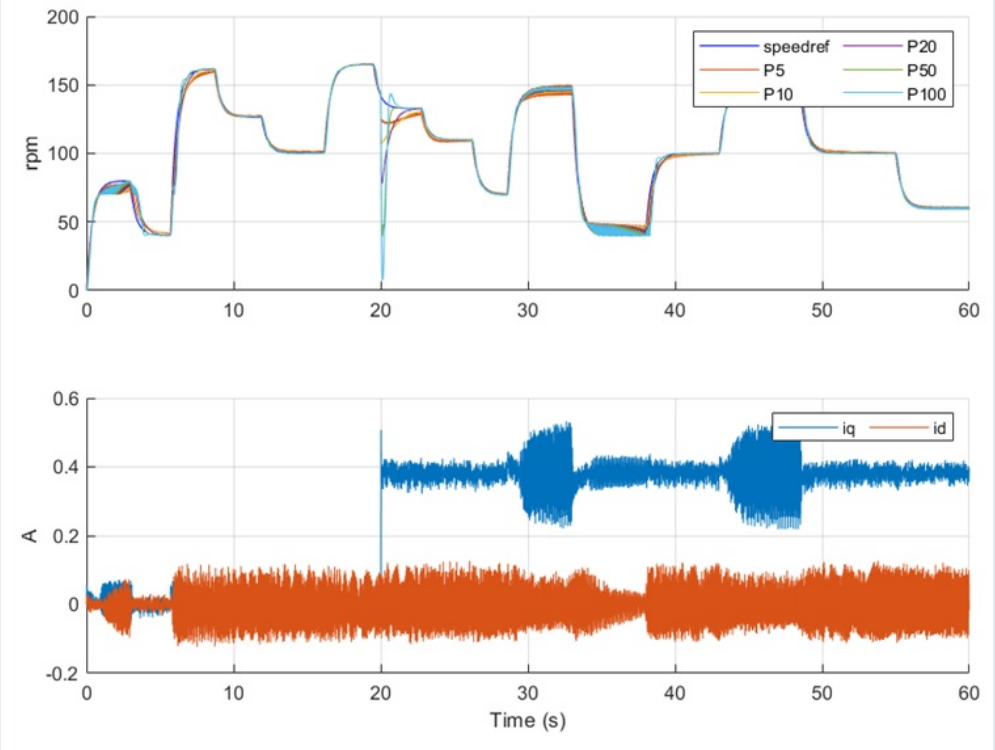

Figure 5: Systematic response survey response affected by parameter PID changing *P3*

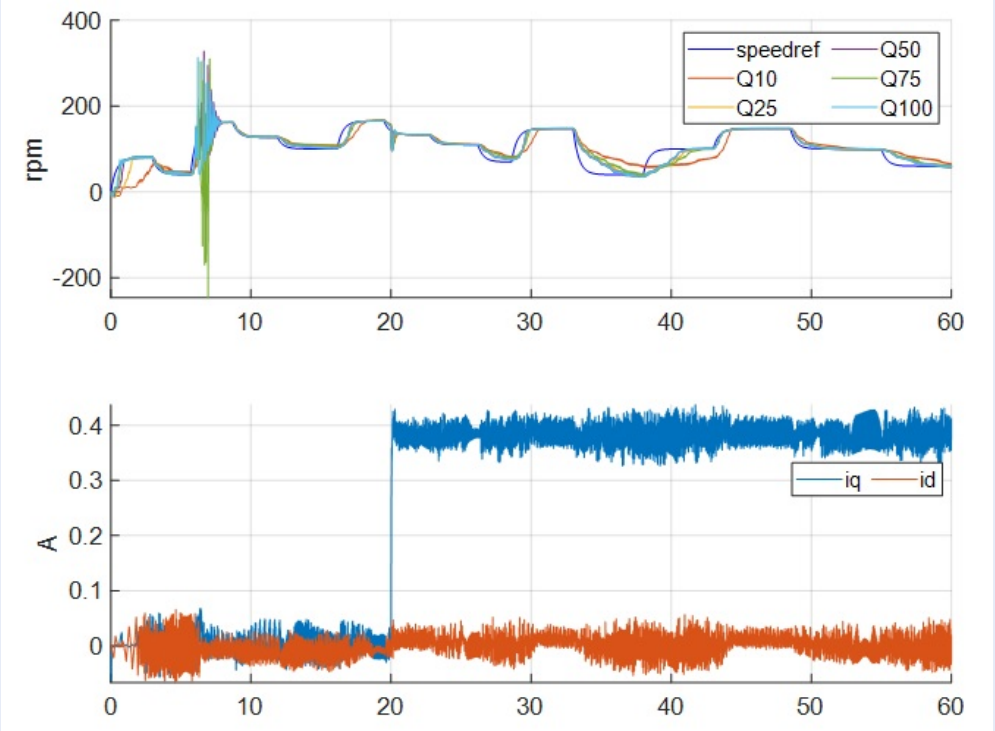

Figure 6: Systematic response survey table affected by parameter Q_a^{-1}, Q_b^{-1}

Table 4: Systematic response survey table affected by parameter $\overline{\delta_a(X)}$, $\overline{\delta_b(X)}$

Case Par	1	2	3	4	5
K_{pq}	20	20	20	20	20
K_{pd}	15	15	15	15	15
K_{iq}	2	2	2	2	2
K_{id}	1	1	1	1	1
Q_a^{-1}	50	50	50	50	50
Q_b^{-1}	50	50	50	50	50
$b(x)$	0.4	0.4	0.4	0.4	0.4
$\overline{\delta_a(X)}$	0.005	0.01	0.06	0.1	1
$\overline{\delta_b(X)}$	0.005	0.01	0.06	0.1	1

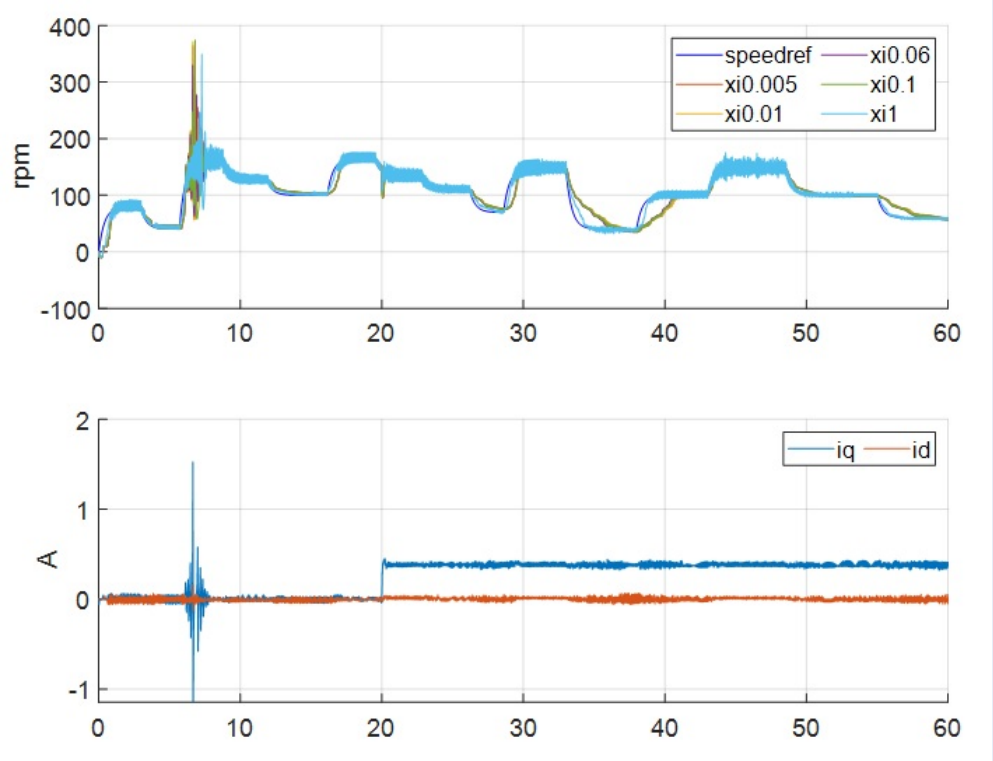

Figure 7: Systematic response survey table affected by parameter $\overline{\delta_a(X)}$, $\overline{\delta_b(X)}$

These results confirm that the erroneous value of PMSM velocity curve has been quite improved via ANSMC. The resulting erroneous value evidently presents that the PMSM velocity regulated by the ANSMC yields convincing results in comparison with other advanced controllers, containing optimal PID and standard SMC approaches.

with K_{pd} K_{id} K_{pq} K_{iq} represent the parameters of the current controller.

The parameters Q_a^{-1}, Q_b^{-1} are selected based on the formula (2-17)

The parameters $b(x)\overline{\delta_a(X)}\overline{\delta_b(X)}$ are chosen using the formula (2-19)

Figure 8 shows that the PMSM real velocity well tracks the desired curve using controller parameters in Table 5. In case an abrupt load at t = 25 seconds in Figure 8 issues the PMSM parameters to be varied, then the proposed ANSMC quickly adapts to this variation and ensures the real velocity to accurately track the desired velocity accurately.

The fact is that the weight of the Lyapunov function Q_a, Q_b decisively affects the adaptive speed of the controller. If Q_a, Q_b large, the system adapts slowly; conversely, if it is small, the system adapts faster, but in this case, the system will also become very sensitive to noise.

In summary, the test results were fully illustrated in Figure 8, with the desired curve of PMSM speed in the blue line and the real PMSM motor velocity in the red with PID control, in the purple in the ANSMC, and the orange in SMC approach. The resulted figure shows that the suggested ANSMC gives a perfect velocity response compared of two other advanced control approaches. Not only that, it is clear to see the steady erroneous value of PMSM velocity response is also perfectly ameliorated. The erroneous value figure shows that the PMSM adjusted by the ANSMC yields good results in comparison with other control methods, such as optimal PID and sliding mode control techniques.

CONCLUSIONS

This study attains scientific significance since it offers both simulation and experimental foundations for comparing and evaluating the efficacy of comparatively advanced control techniques applied to PMSM velocity regulation. The suggested ANSMC control methodology yields perfect results in comparison with other traditional control methods like field-oriented FOC-PID and SMC PMSM speed control techniques. The topic's practical significance lies in its ability to address the issues of PMSM speed control, a prevalent problem with widespread applications. Concerning the restriction of this study, in the future, we can produce advanced steering circuits for application in conveyor belts and electric vehicles EV based on these contributions.

ACKNOWLEDGEMENT

This research is funded by Vietnam National Foundation for Science and Technology Development (NAFOSTED), Vietnam, under grant number 107.01-2021.22.

CONFLICT OF INTEREST

The authors confirm that there is not any conflict of interest related to the content reported in this paper.

AUTHORS' CONTRIBUTION

Nguyen Tien Dat: Conceptualization, Formal analysis, Investigation, Methodology, Resources, Supervision, Validation, Visualization, Writing – review & editing.

Ho Pham Huy Anh: Funding acquisition, Project administration, Supervision, Vali-dation, Writing – review & editing.

REFERENCES

1. Casadei D, Frede Blaabjerg, Hansen S. FOC and DTC: two viable schemes for induction motors torque control. IEEE transactions on Power Electronics. 2002;17(5):779-787;Available from: https://doi.org/10.1109/TPEL.2002.802183.
2. Wang L, Tian M, Gao Y. Fuzzy self-adapting PID control of PMSM servo system. In: 2007 IEEE International Electric Machines & Drives Conference. IEEE; 2007. p. 860-863;Available from: https://doi.org/10.1109/IEMDC.2007.382781.
3. Hu H. Optimal PID controller design in PMSM servo system via particle swarm optimization. In: 31st Conf. of IEEE Ind. Electronics Society, IECON 2005. IEEE; 2005. p. 5;.
4. Xi X, Yongdong L, Min L. Performance control of PMSM drives using a self-tuning PID. In: IEEE International Conference on Electric Machines and Drives. IEEE; 2005. p. 1053-1057;.
5. Junli G, Yingfan Z. Research on parameter identification and PI self-tuning of PMSM. In: The 2nd International Conference on Information Science and Engineering. IEEE; 2010. p. 5251-5254;.
6. Zang B, Li Y. A PMSM sliding mode control system based on model reference adaptive control. In: IPEMC-2000. The 3rd Inter. Power Electronics Conference. IEEE; 2000. p. 336-341;.
7. Saihi L, et al. A robust sensorless SMC of PMSM based on sliding mode observer and extended Kalman filter. In: 2015 4th International Conference on Electrical Engineering (ICEE). IEEE; 2015. p. 1-4;Available from: https://doi.org/10.1109/INTEE.2015.7416838.
8. Yanxia S, Dinghui W, Zhicheng J. Model reference fuzzy adaptive control of permanent magnet synchronous motor. In: Chinese Control Conference; 2006;Available from: https://doi.org/10.1109/CHICC.2006.280747.
9. El-Sousy FFM. High-performance neural-network model-following speed controller for vector-controlled PMSM drive system. In: 2004 IEEE International Conference on Industrial Technology, IEEE ICIT'04. IEEE; 2004. p. 418-424;.
10. Kumar R, Gupta RA, Bansal AK. Identification and control of PMSM using artificial neural network. In: 2007 IEEE International Symposium on Industrial Electronics. IEEE; 2007. p. 30-35;Available from: https://doi.org/10.1109/ISIE.2007.4374567.

Table 5: Proposed ANSMC controller parameters

Coefficient	Magnitude
K_{pq}	5.19
K_{pd}	2.28
K_{iq}	5.41
K_{id}	1.61
Q_a^{-1}	50.0
Q_b^{-1}	50.0
$b(x)$	0.4
$\overline{\delta_a(X)}$	0.06
$\overline{\delta_b(X)}$	0.04

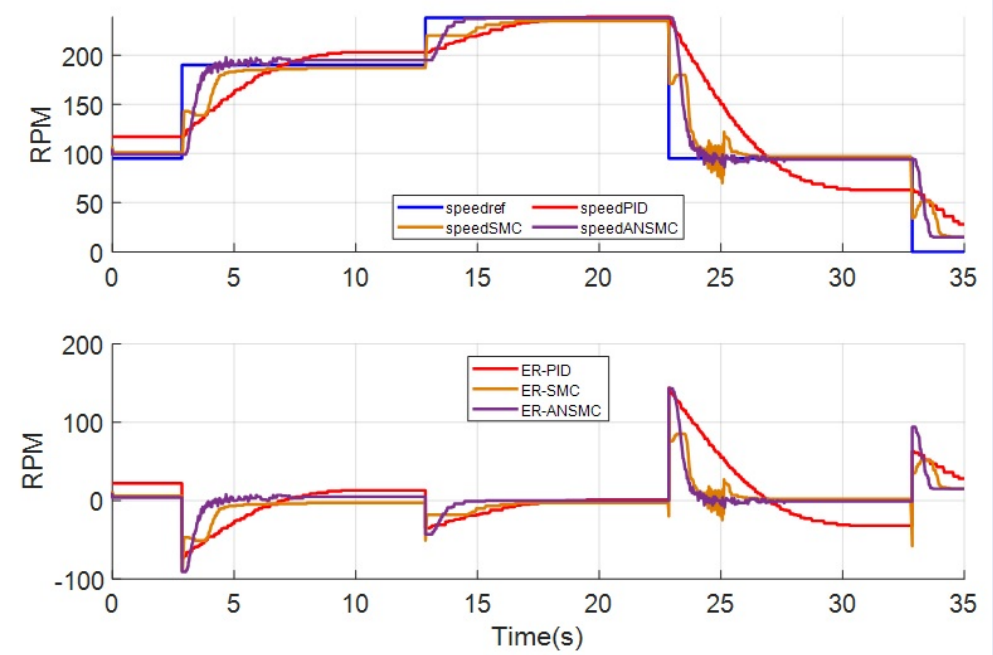

Figure 8: Comparative PMSM motor velocity performance

11. Xi X, Yongdong L, Min L. Performance control of PMSM drives using a self-tuning PID. In: IEEE International Conference on Electric Machines and Drives. IEEE; 2005. p. 1053-1057;.
12. Zhang X, et al. Nonlinear speed control for PMSM system using sliding-mode control and disturbance compensation techniques. IEEE Transactions on Power Electronics. 2012;28(3):1358-1365;Available from: https://doi.org/10.1109/TPEL.2012.2206610.
13. Li S, Gu H. Fuzzy adaptive internal model control schemes for PMSM speed-regulation system. IEEE Transactions on Industrial Informatics. 2012;8(4):767-779;Available from: https://doi.org/10.1109/TII.2012.2205581.
14. Luy TN, Cong TP, Cong DP. Neural network observers and sensorless robust optimal control for partially unknown PMSM with disturbances and saturating voltages. IEEE Transactions on Power Electronics. 2021;36(10):12045-12056;Available from: https://doi.org/10.1109/TPEL.2021.3071465.
15. Jankowska K, et al. Design and Analysis of Current Sensor Fault Detection Mechanisms for PMSM Drives Based on Neural Networks. Designs. 2022;6(1):18;Available from: https://doi.org/10.3390/designs6010018.
16. El-Sousy FFM, Alenizi FAF. Optimal Adaptive Super-Twisting Sliding-Mode Control Using Online Actor-Critic Neural Networks for Permanent-Magnet Synchronous Motor Drives. IEEE Access. 2021;9:82508-82534;Available from: https://doi.org/10.1109/ACCESS.2021.3086423.
17. Junejo AK, et al. Adaptive speed control of PMSM drive system based a new sliding-mode reaching law. IEEE Transactions on Power Electronics. 2020;35(11):12110-12121;Available from: https://doi.org/10.1109/TPEL.2020.2986893.
18. Murali A, et al. Assessing finite control set model predictive speed controlled PMSM performance for

deployment in electric vehicles. World Electric Vehicle Journal. 2021;12(1):41;Available from: https://doi.org/10.3390/wevj12010041.
19. Shanthi R, Kalyani S, Devie PM. Design and performance analysis of adaptive neuro-fuzzy controller for speed control of permanent magnet synchronous motor drive. Soft Computing. 2021;25:1519-1533;Available from: https://doi.org/10.1007/s00500-020-05236-5.
20. Suleimenov K, Do TD. A practical disturbance rejection control scheme for permanent magnet synchronous motors. Symmetry. 2022;14(9):1873;Available from: https://doi.org/10.3390/sym14091873.
21. Nguyen HV, et al. Dynamical Delay Unification of Disturbance Observation Techniques for PMSM Drives Control. IEEE/ASME Transactions on Mechatronics. 2022;27(6):5560-5571;Available from: https://doi.org/10.1109/TMECH.2022.3181176.
22. Suleimenov K, Do TD. Design and Analysis of a Generalized High-Order Disturbance Observer for PMSMs With a Fuzzy-PI Speed Controller. IEEE Access. 2022;10:42252-42260;Available from: https://doi.org/10.1109/ACCESS.2022.3167429.
23. Sarsembayev B, Suleimenov K, Do TD. High order disturbance observer based PI-PI control system with tracking anti-windup technique for improvement of transient performance of PMSM. IEEE Access. 2021;9:66323-66334;Available from: https://doi.org/10.1109/ACCESS.2021.3074661.

Tạp chí Phát t riển Khoa học và Công nghệ – Kĩ thuật và Công nghệ 2023, 6(4):2048-2059

Open Access Full Text Article

Bài nghiên cứu

Điều khiển trượt thích nghi dùng mạng nơ rôn với hàm cơ sở xuyên tâm áp dụng trong động cơ đồng bộ ba pha

Nguyễn Tiến Đạt[1,2], Hồ Phạm Huy Ánh[1,2,*]

TÓM TẮT

Trong các ứng dụng thực tế, động cơ đồng bộ nam châm vĩnh cửu có nhiều lợi ích hơn động cơ loại chổi than, chẳng hạn như thiết kế nhỏ gọn, tỷ lệ mô-men xoắn và quán tính cao, mật độ công suất cao, mật độ từ thông khe hở không khí cao và hiệu suất cao. Hơn nữa trong xu hướng gần đây, chúng cũng thay thế động cơ cảm ứng trong nhiều lĩnh vực ứng dụng. Phản ứng nhanh, điều khiển chính xác và giảm thiểu độ vọt lố trong chất lượng điều khiển và những yếu tố quan trọng được cân nhắc trong quy trình phát triển và thiết kế hệ thống điều khiển cho các ứng dụng động cơ đồng bộ nam châm vĩnh cửu. Các mô hình động cơ đồng bộ nam châm vĩnh cửu là mô hình phi tuyến và bậc cao liên quan đến các tham số thay đổi theo thời gian, do đó cần có bộ điều khiển phù hợp. Một kỹ thuật điều khiển dựa trên mô hình toán của đối tượng rất phổ biến dành cho các hệ thống có tham số dao động và nhiễu bên ngoài là điều khiển chế độ trượt. Đầu tiên, bộ điều khiển chế độ trượt được sử dụng để giảm rung lắc và ổn định hệ thống truyền động PMSM. Mặt khác, việc sửa đổi cấu hình hệ thống truyền động và các nhiễu loạn bên ngoài có thể phá hủy hoàn toàn hiệu suất điều khiển. Vì thế,Bài báo này nghiên cứu việc kết hợp mạng lưới nơ rôn với kỹ thuật chế độ trượt để đề xuất thuật toán điều khiển tốc độ động cơ đồng bộ nam châm vĩnh cửu mạnh mẽ tiên tiến. Để tăng tính mạnh mẽ, ổn định và giảm rung lắc chế độ trượt của bộ điều khiển, mục tiêu của chúng tôi là giới thiệu một số thiết kế luật thích ứng để cập nhật luật điều khiển chế độ trượt trực tuyến và thiết kế bộ điều khiển tổng hợp sử dụng mạng nơ ron với hàm cơ sở xuyên tâm. Bộ điều khiển chế độ trượt mạng nơron thích ứng được đề xuất dựa trên sơ đồ định hướng trường được viết tắt là kỹ thuật ANSMC-FOC, hay còn được gọi là chế độ trượt nơ rôn thích nghi dựa trên phương pháp điều khiển hướng trường, đã khẳng định độ chính xác hoàn toàn của nó và đạt được hiệu suất điều khiển vượt trội so với PID và phương pháp điều khiển trượt cổ điển. Do đó, thuật toán điều khiển tốc độ động cơ đồng bộ nam châm vĩnh cửu được đề xuất tốt hơn một cách thuyết phục so với các phương pháp điều khiển tốc độ tiên tiến của động cơ đồng bộ nam châm vĩnh cửu khác.

Từ khoá: Điều khiển trượt thích nghi (SMC), Động cơ đồng bộ nam châm vĩnh cửu (PMSM), Điều khiển hướng trường (FOC), Mô hình mạng nơ rôn hàm cơ sở xuyên tâm thích nghi, Điều khiển PID, Điều khiển trượt thích nghi dùng mạng nơ rôn thích ứng dựa trên mô hình điều khiển hướng trường (ANSMC-FOC/ANSMC)

[1]*Trường Đại học Bách khoa (HCMUT), số 268 Lý Thường Kiệt, Quận 10, TP.HCM, Việt Nam*

[2]*Đại học Quốc gia Thành phố Hồ Chí Minh (VNU-HCM), Phường Linh Trung, TP. Thủ Đức, TP.HCM, Việt Nam*

Liên hệ

Hồ Phạm Huy Ánh, Trường Đại học Bách khoa (HCMUT), số 268 Lý Thường Kiệt, Quận 10, TP.HCM, Việt Nam

Đại học Quốc gia Thành phố Hồ Chí Minh (VNU-HCM), Phường Linh Trung, TP. Thủ Đức, TP.HCM, Việt Nam

Email: hphanh@hcmut.edu.vn

Lịch sử

- Ngày nhận: 07-12-2022
- Ngày chấp nhận: 27-3-2024
- Ngày đăng: 13-5-2024

DOI : https://doi.org/10.32508/stdjet.v6i4.1057

VNUHCM PRESS

Trích dẫn bài báo này: Đạt N T, Ánh H P H. **Điều khiển trượt thích nghi dùng mạng nơ rôn với hàm cơ sở xuyên tâm áp dụng trong động cơ đồng bộ ba pha**. *Sci. Tech. Dev. J. - Eng. Tech.* 2023, 6(4):2048-2059